Transient plasma ignition for clean, fuel-efficient, transportation vehicle engines

Final Report

METRANS project 07-20

Reporting Period: September 2006 – August 2008

Prof. Paul D. Ronney, Principal investigator
Prof. Martin Gundersen, co-investigator

University of Southern California
Department of Aerospace and Mechanical Engineering
Olin Hall of Engineering 430
Los Angeles, CA 90089

Disclaimer

The contents of this report reflect the views of the authors, who are responsible for the facts and the accuracy of the information presented herein. This document is disseminated under the sponsorship of the Department of Transportation, University Transportation Centers Program, and California Department of Transportation in the interest of information exchange. The U.S. Government and California Department of Transportation assume no liability for the contents or use thereof. The contents do not necessarily reflect the official views or policies of the State of California or the Department of Transportation. This report does not constitute a standard, specification, or regulation.

Abstract

The use of non-thermal transient plasma ignition (TPI) as an alternative to spark ignition (SI) for internal combustion engines was investigated. A 2.5 liter 4-cylinder test engine was used that has two spark plug ports per cylinder to enable direct, instantaneous and valid comparisons of spark and corona ignition at the same time under identical engine operating conditions. A ceramic corona electrode was designed that fits in the new test engine and is capable of withstanding the pressures and temperatures encountered inside the combustion chamber. The corona ignition system was tested on the engine and an increase (compared to spark ignition) in both peak pressures and indicated mean effective pressure (IMEP) were observed. Testing showed typically 15 - 20% increases in IMEP and much shorter burn durations at identical operating conditions. Moreover, the tradeoff between thermal efficiency and brake specific NOx emissions was found to improve with TPI. It is proposed that these advantages of corona ignition may be exploited by either (1) the use of leaner fuel-air ratios or (2) by designing engines with lower turbulence levels, thereby reducing heat loss to cylinder walls and increasing thermal efficiency, and employing corona ignition to obtain sufficiently rapid burning.

List of figures and tables

Table of contents

1 Introduction

The electric arc has been the ignition source of choice for automotive combustion engines for over 100 years. It has many advantages including simplicity, low cost, size and weight of the electronics, and it produces sufficiently high temperatures to dissociate and partially ionize most fuel and oxidant molecules. Nevertheless, there are also numerous disadvantages of arc discharges, including the limited size of the discharge, the low energy of the electrons that are created and the low "wall-plug" efficiency (*i.e.*, ratio of energy deposited in the gas to the electrical energy consumed in producing the discharge.) For these reasons, many investigations of ignition by laser sources have been conducted in recent years. Still, laser ignition sources present many practical difficulties, especially the need for reliable, low-attenuation optical access, extremely low wall-plug efficiency, and extremely high optical intensities needed to induced breakdown in the gas which in turn makes it difficult to control the location and intensity of the discharge.

In the proposed investigation *transient plasma discharges* (sometimes called *pulsed corona discharges*) will be used for the initiation of combustion in low-turbulence premixed-charge internal combustion engines to "restore" burning rate lost by reduction of turbulence levels. The transient plasma discharge is defined as the portion of an electric discharge before the onset of the low-voltage, high current arc discharge. Only the earliest, most efficient transient plasma discharge stage, is used for ignition. The discharge is stopped before the later, less efficient (and geometrically less desirable) stage begins. The electrical energy that would have been used in these later inefficient stages is saved for the next combustion cycle.

With recent advances in pulsed power electronics developed at USC, for the first time transient plasma discharges can be produced with very high wall-plug energy efficiencies in a system of reasonable cost, size and weight. Effectively these electronics produces only the transient plasma phase of the discharge; the later arc discharge is a less efficient source for transferring energy to ionization, electronic excitation, and dissociation, does not occur, and thus less energy is required for a given ignition event. Consequently, in addition to the inherent increase in burn rate possible with transient plasma ignition, the transient plasma generators proposed here are much more energy-efficient than any advanced ignition system producing arc-type discharges, and thus introduce less parasitic losses in terms of the shaft power needed to drive the electrical generator supplying the ignition system. Furthermore, we note that there is much less heating and erosion of the electrodes in the transient plasma phase than in the arc phase and thus transient plasma ignition systems are likely to be more reliable than conventional ignition systems.

It should be emphasized that the transient plasma discharges discussed here are entirely different from that used in any prior IC engine studies outside of our group and cannot be produced by conventional IC engine ignition systems. Unlike so-called "plasma igniter" spark plugs that have been around for many years, which simply produce and expel a minute amount of low energy electrons a short distance, the transient plasma generator produces streamers of high energy electrons that span the entire combustion chamber volume and are generated with high wall-plug efficiencies.

Consequently, the objective of the current work was to assess the feasibility of employing pulsed corona discharges in internal combustion engines. Initially, burn-rate measurements were made in constant-volume chambers under quiescent and turbulent condition, comparing spark-ignited and corona-ignited flames. Based on these encouraging results, performance in a laboratory engine was measured, again comparing conventional ignition to corona discharge ignition.

2 Experimental Apparatus

2.1 Corona Generator

The experimental apparatus for the constant-volume tests consists of an electronic system to generate pulsed corona discharges and a combustion cylinder with measurement and gas handling system (Fig. 1). The pulsed power includes a high voltage pulse generator utilizing a thyratron (Triton F-211) and a Blumlein transmission line to create a high voltage pulse (typically 30 - 60 kV) with narrow pulse width (typically 100 nsec). The maximum pulse energy employed was 1.8 J. For engine tests a pseudospark-switched circuit having higher repetition rate capability was used instead of the thyratron circuit. All signals were displayed and recorded by a digital oscilloscope (Tektronix TDS 420A).

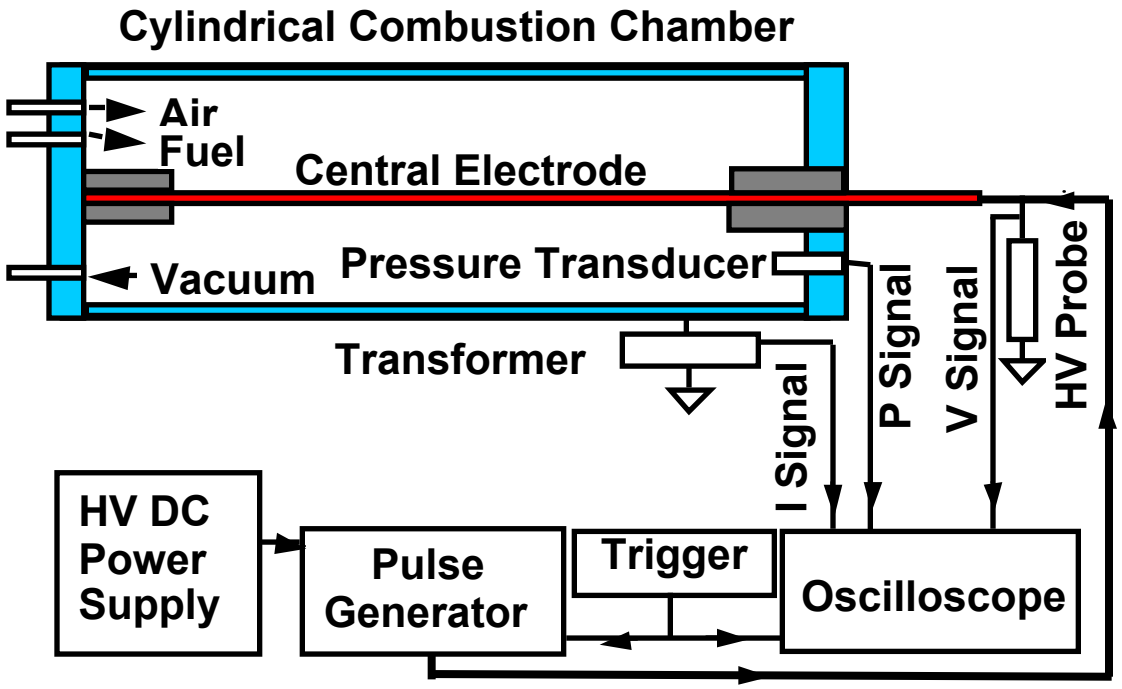

Figure 1. Experiment setup for investigation of flame ignition by pulsed corona discharge

The same equipment is used in static combustion chambers and in the engine experiments. The firing is triggered at the desired timing from an optical encoder on the engine.

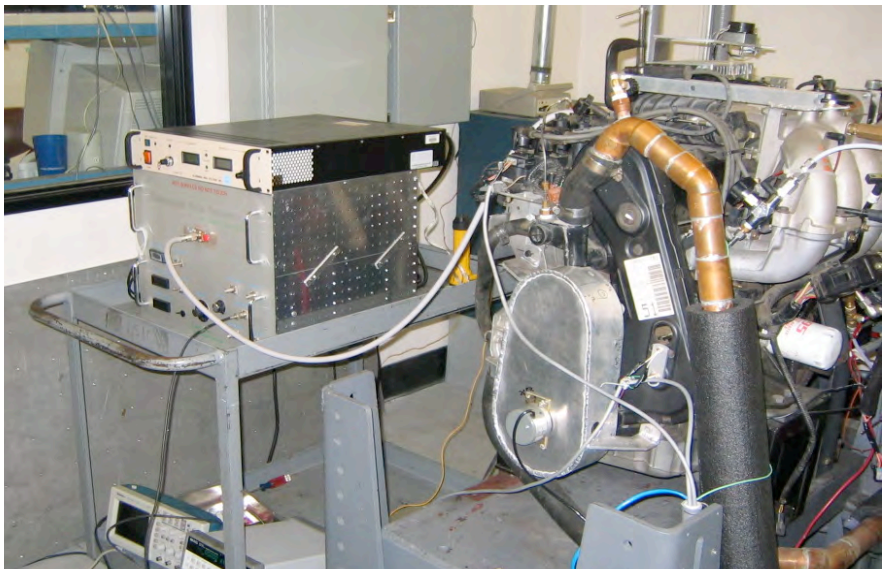

Figure 2. Corona generator connected to one cylinder on test engine

2.2 Test Chambers

Three different test chambers have been developed for testing of the corona discharge ignition. The first test cylinder is constructed from a 2.5" ID stainless steel tube that acts as the ground electrode. This chamber has an interchangeable metal rod placed at its central axis acting as the (central) electrode. The outer electrode is always grounded and the central electrode is connected to high voltage. In this report all reported experiments were done with positive corona (central electrode is anode) unless otherwise noted. There are gas inlets, outlet and vacuum pump inlet in one end plate and pressure gauge (Omega, DPG1000B), pressure transducer (Omega PX4201) and conventional car sparkplug (Bosch, platinum) on the other end plate. The sparkplug was switched by a standard automotive ignition circuit. A transparent plastic end plate was used for end view photos. This chamber also has a configuration that allows for testing under turbulent conditions (See Fig. 3).

The second test chamber used for the corona ignition experiments was modeled after the dimensions of the combustion chamber in the test engine. This chamber was constructed from 6061 T6 aluminum and consists of a bottom half that is machined into the shape of the piston dome of the test engine, and a top half that is machined to closely match the volume of the cylinder head. The two pieces are bolted together with six 5/16" bolts and are sealed with an O-ring (seen in Figs. 6 and 7). With this test chamber various electrode shapes and configurations could be tested much more quickly than in the engine. For tests performed at 1 atmosphere, the corona generator and the measurement equipment are identical to those used with the cylindrical shaped chamber. For tests run at elevated pressures a Kistler model 603B1 spark plug-mounted pressure transducer and model 5004 dual mode amplifier were used to measure the pressure. When performing ignition tests in this chamber the gas and air mixture was premixed in a larger chamber (Fig. 4). Combustion tests were performed at initial pressures up to 9.5 atmospheres. An alternate chamber top plate was fabricated from a ¼" plate of aluminum that leaves the sides open for photographing the test chamber (Fig. 7).

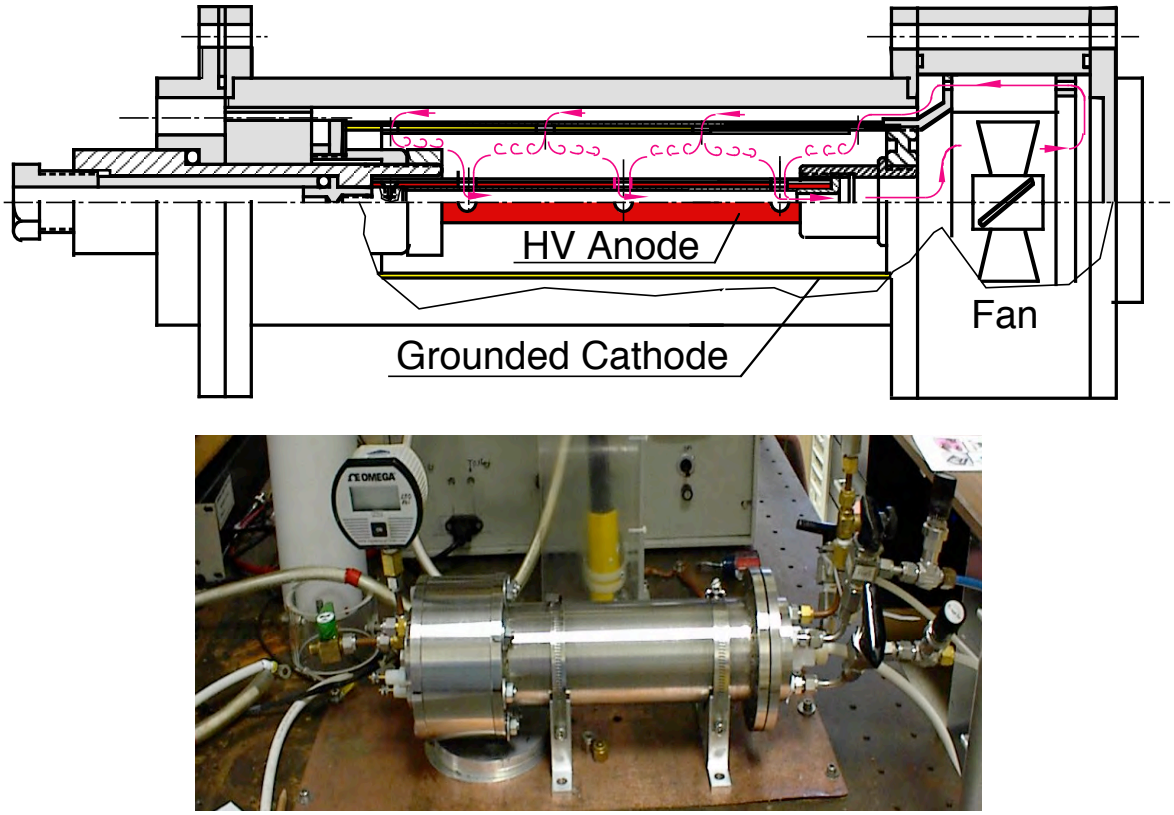

Figure 3. Top: Cutaway diagram of turbulent test chamber; bottom: photograph of chamber

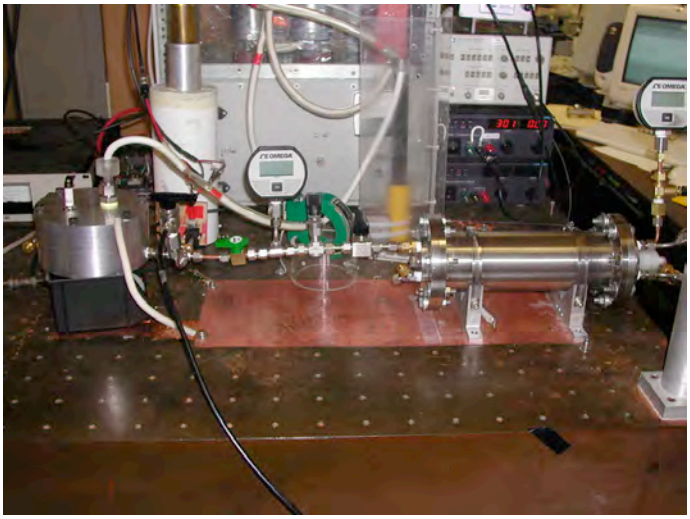

Figure 4. Experimental setup for engine cylinder test chamber

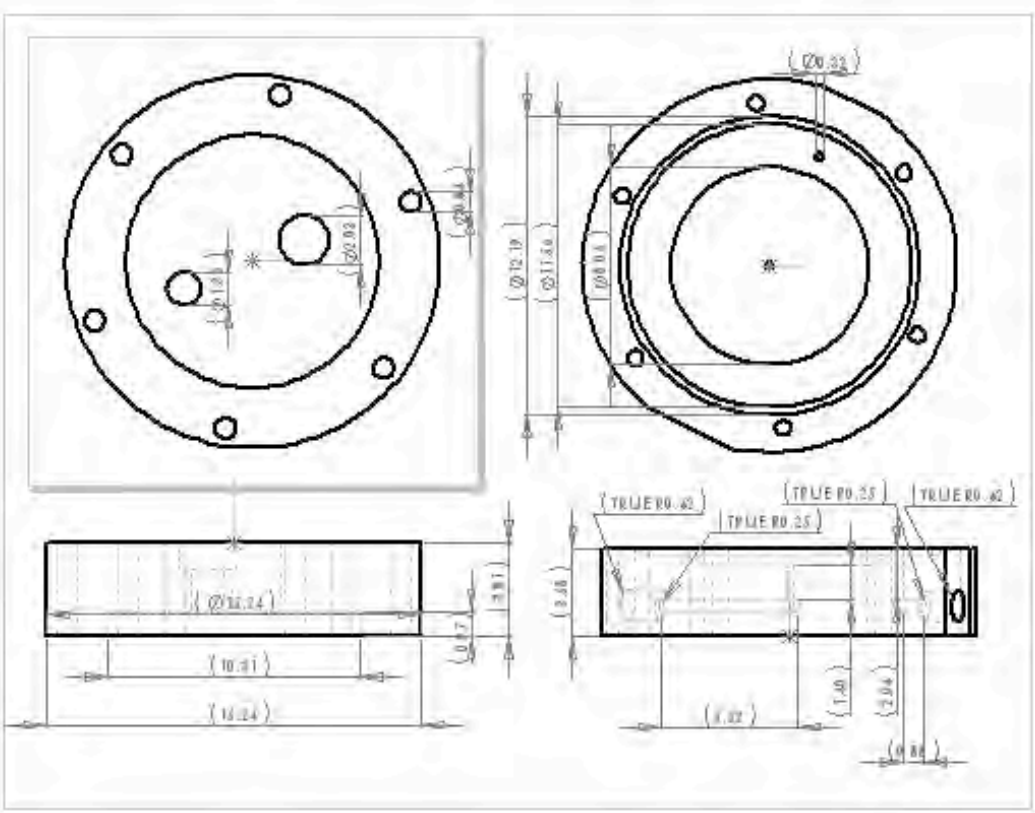

Figure 5. Dimensioned drawing of Engine Cylinder Test Chamber

Figure 6. Exploded view of Engine Cylinder Test chamber assembly, shown with circular ring electrode

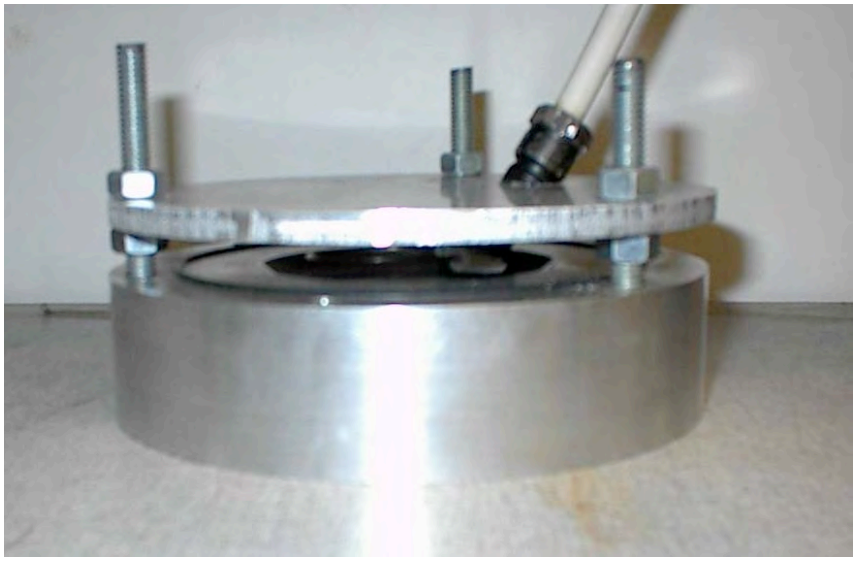

Figure 7. Engine cylinder test chamber in open configuration for visualizing corona discharges.

The third test chamber used in testing is constructed using a cylinder head and piston from the test engine described in below in section C. An aluminum block was machined to accept the piston from the test engine and holds the piston in a TDC position (see Fig. 9). The block has four holes that are tapped to accept the head bolts that secure the piston/block assembly to the head. The seal between the head and the block is held by using a head gasket from the engine. Gas handling is done through fittings installed in block-off plates that are installed over the intake and exhaust ports. Measurements are done with the same equipment used on the other test chambers. This chamber allows electrodes to be tested in a chamber with the exact same dimensions of the engine.

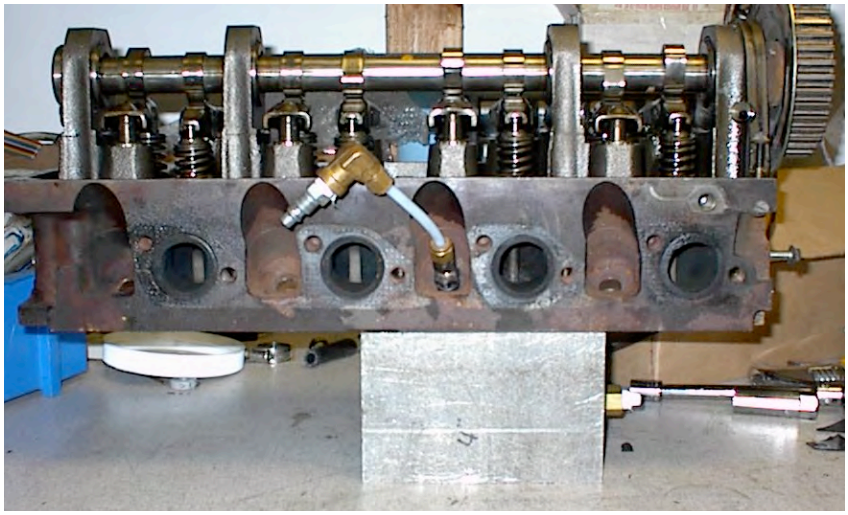

Figure 8. Test chamber using piston and cylinder head from engine (assembled).

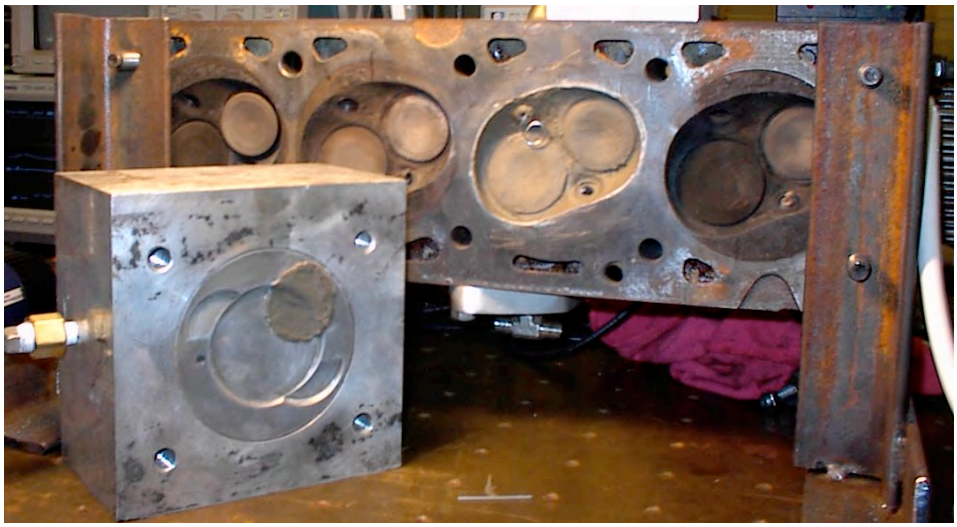

Figure 9. Test chamber using piston and cylinder head from engine (disassembled).

2.3 Dual Plug Test Engine and Instrumentation

The test engine as seen in Figure 10 was required to simplify the testing of the corona discharge ignition system in the engine. The engine purchased was a 2.5 liter 4 cylinder engine from a 2000 Ford Ranger Pickup. This engine was chosen because it has two spark plug ports per cylinder. This allows the corona electrode to be inserted into one of the ports and a conventional spark plug with cylinder pressure transducer to be inserted in the other. The engine was adapted to run on natural gas using a control valve and natural gas flow meter.

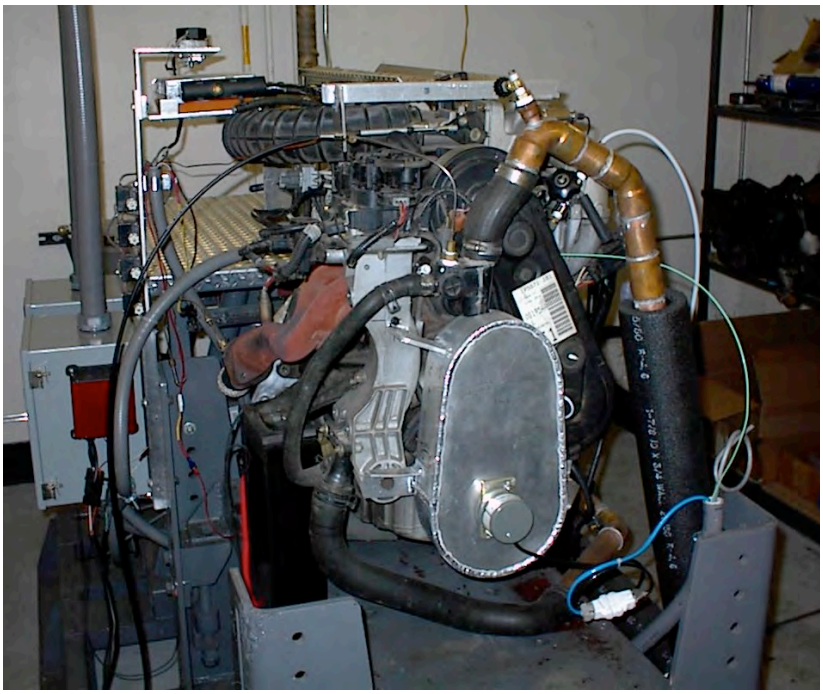

Figure 10. Test engine mounted to dynamometer.

Figure 11. Main panel for data acquisition and control equipment. Top left AMUX-64T, top right SCB-68, bottom left MID-7604, bottom right CB68-LPR

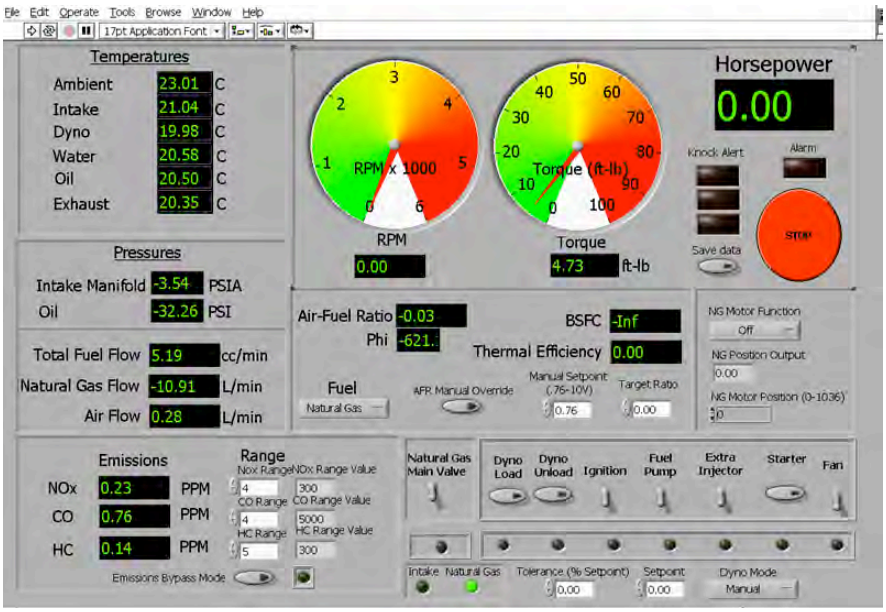

Figure 12. Screen capture of PC engine Control Panel

Data acquisition and control hardware was purchased from National Instruments for the engine lab. This equipment consists of a PCI-6031E DAQ card, a PCI-7344 motion control card, an AMUX-64T terminal block for thermocouple inputs, a SCB-68 terminal block for analog inputs, a MID-7604 stepper motor driver and a CB68-LPR terminal block for digital IO (Fig. 11). The engine is fully instrumented and all critical pressures, temperatures and other parameters are monitored.

Software was developed using LabView to interface with the new hardware. The software displays all of the pertinent engine parameters and incorporates PID control for the air/fuel ratio

and dyno load control. The user interface was developed to be easy to read and user friendly (Fig. 12). Warning alarms and safety shutdowns were incorporated to protect the engine when parameters (pressures, temperatures or speed) get out of a safe range.

2.4 Cylinder Pressure Monitoring System

In order to quantify the performance characteristics of the corona discharge ignition system it was necessary to monitor the pressure of the cylinder that the corona electrode is installed in. A cylinder pressure monitoring system was designed to accomplish this task. The system consists of a Kistler pressure transducer with amplifier, an optical encoder coupled to the crankshaft with 2048 pulses per revolution (providing 0.18 degree resolution), and a high speed data acquisition card from National Instruments (NI 6070E). The amplifier was located in a shielded enclosure as was the terminal block for the wiring connections (Fig. 13).

Figure 13. Control cabinet for cylinder pressure monitoring system

The pressure transducer reads the cylinder pressure through a spark plug that was modified by Kistler with an added port for the transducer as seen in Fig. 14.

A program was created in LabView that collects cylinder pressure traces based on the trigger inputs received from the encoder that is mounted on the crankshaft. Cylinder pressure data is logged vs crank angle. This data is then imported into a spreadsheet where IMEP is calculated and PV diagrams are created.

2.5 Ceramic Corona Electrode

The electrodes that were used for testing the corona in the test chambers were constructed of a plastic that could withstand the pressures of single shot combustion tests but not the temperatures encountered in a running engine. It was necessary to design an electrode that could withstand the temperatures and pressures of a running engine. A conventional spark plug could not be used as the conductor for the corona electrode as the electrical resistance is much too high for this application. The resistance should be as low as possible for the corona electrode to perform properly.

Figure 14. Modified spark plug with pressure transducer installed.

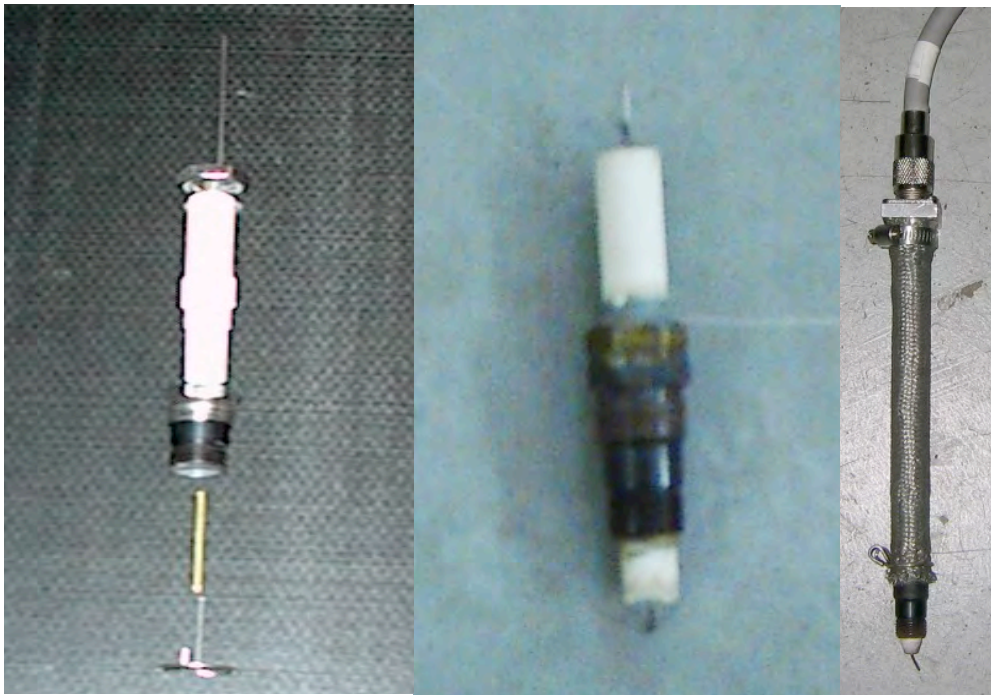

Figure 15. Ceramic corona electrode for running in engine show in exploded view (left), assembled (center) and shielded (right).

A machinable ceramic (Macor™) was chosen that has both high temperature resistance, good electrical insulating properties and is easily machinable. The steel body of the corona electrode uses a spark plug body with the original ceramic portion removed. The swaged lip was machined off the body that holds the ceramic in place. The Macor is purchased in ½" diameter rods and

machined down to fit the steel spark plug casing. A shoulder is machined into the top of the ceramic rod which is captured by a steel ring installed from the top which is then welded to the spark plug body. A 1/8" brass rod is drilled from both ends to accept the electrode tip and the conductor. The brass rod is installed from the bottom and is held in place with a high temperature epoxy. This design allows different electrode tips to be used with one electrode body. The electrodes were hydro-tested at 1000 psi before put service in the engine.

3 Results

3.1 Electrical Characteristics

Photographs of various pulsed corona discharge are shown in Figs. 17 and 18. They were taken in a completely dark environment. Fig. 17 is a pulsed corona discharge with a plain electrode viewing from the end of cylindrical chamber. This shows many streamers distributed along the length of central electrode and superimposed with each other. If viewed from side many discrete streamers evenly distributed on the surface of the central electrode are evident. The average separation between streamers is 5mm and average diameter is 0.7mm. An estimated number of streamers on the central electrode is 600. When pulse energy was reduced from 356mJ/pulse to 44mJ/pulse the total number of streamers did not change noticeably, but the brightness of streamers decreased. Figure 18 shows the corona discharge from the side view in the open top chamber as seen in Fig. 7.

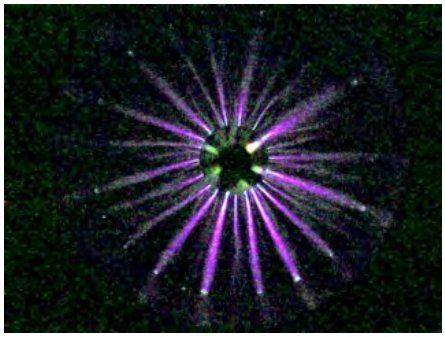

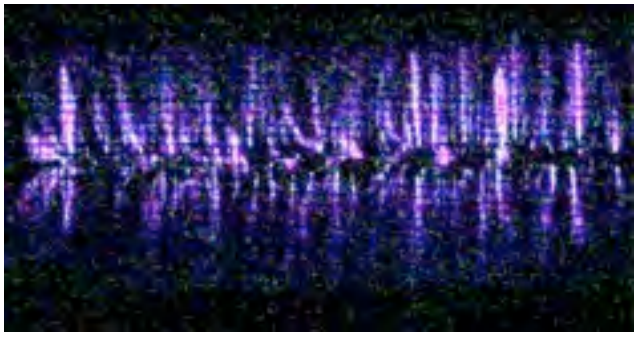

Figure 16. Picture of pulsed corona discharge (end view). Diameter of central electrode: 6.35mm, energy: 251 mJ.
Figure 17. Picture of pulsed corona discharge (side view). Diameter of central electrode: 6.35mm , energy: 356 mJ.

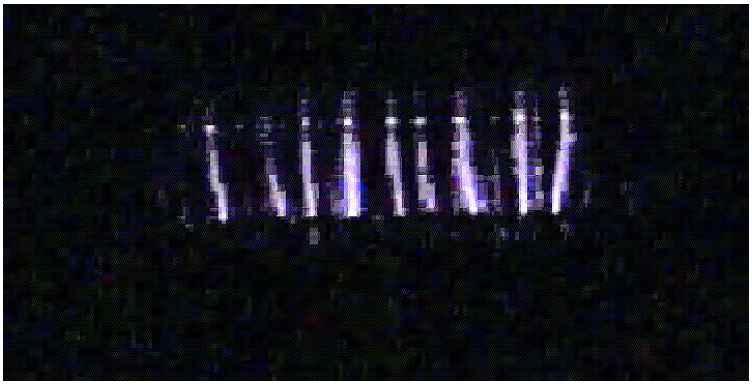

Figure 18. Photograph of corona discharge in engine cylinder test chamber with open top plate installed. .5mm diameter electrode 50mm circular ring

Figures 19 and 20 shows typical voltage, current and energy waveforms of pulsed corona discharges with and without arcing. Current waveforms clearly show the difference between corona discharges with arcing and without arcing. Both dashed and solid curves have a first peak that corresponds to the corona discharge. Only the dash curve has the second current peak which correspondences to arc discharge. One can see that after arcing (at 150 ns after trig where current started to rise rapidly) voltage drops rapidly. Consequently, no rapid energy increase was observed on energy waveform implying that arcing does not contribute significantly to energy input to plasma at the voltages at which arc is going to start, during times on the order of 100s of nanoseconds. In these experiments the experimental conditions (mainly the applied voltage and electrode structure) were so controlled that no arcs were observed to ensure that only the transient phase occurred before the formation of arcing. Typical voltage pulse width (FWHM) is 140 ns, and current pulse width 80 ns.

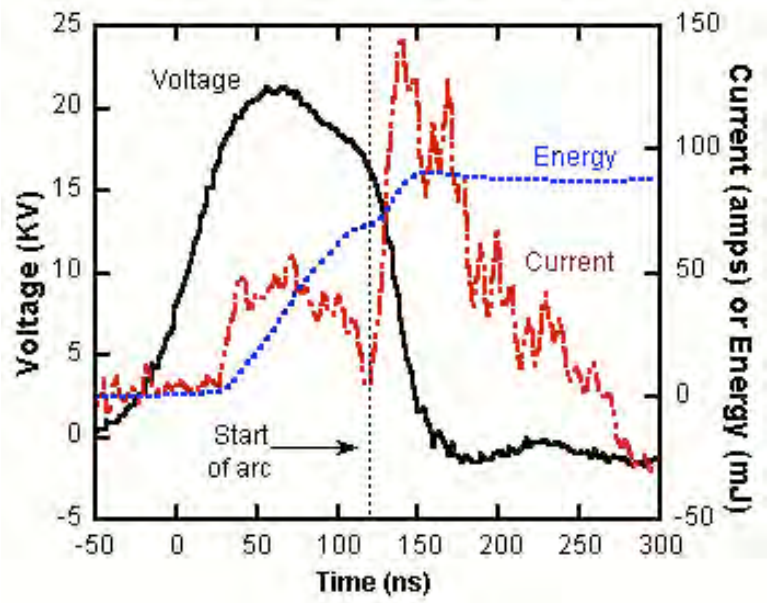

Figure 19. Plot of voltage, energy and current delivered to the gas for corona discharge plus arc. Test performed in engine cylinder test chamber.

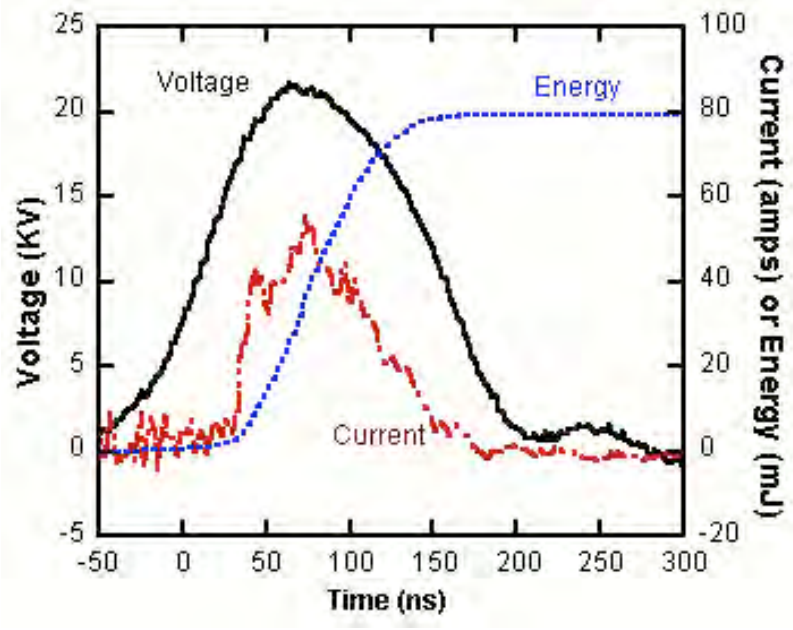

Figure 20. Plot of Voltage, Energy and Current delivered to the gas for corona discharge only. Test performed in engine cylinder test chamber.

Pulse energy as a function of peak voltage was measured for various electrodes. The pulse energy increases non-linearly and is faster at higher peak voltages. There is an intercept peak voltage, below which no energy output to plasma, i.e. pulse corona discharge starts at a certain value of peak voltage. The intercept peak voltage decreases as decreasing of diameter of central electrode. At the same peak voltage, a thinner central electrode provides higher pulse energy than a thick central electrode does. A threaded electrode produces higher pulse energy than smooth electrode (plain electrode) with the same diameter and peak voltage. In our particular conditions, brush-like electrodes provide best electrical performance. Positive corona discharge (central electrode is anode) is much better than negative corona discharge (central electrode is cathode). In the experiments reported below, only positive pulsed corona discharge is used.

3.2 Combustion Characteristics

The experimental procedure for bench testing the corona discharge in the test chambers were as follows. The test cylinder was evacuated with a vacuum pump until the pressure was less than 0.01 psi. Then fuel (CP grade) and air (dry cylinder air) were filled into the cylinder using the partial pressure method. Composition was controlled with a digital pressure gauge with precision of 0.01 psi. After igniting with either pulsed corona or spark discharge, the pressure was measured by the pressure transducer. Pressure signals were read and recorded by the digital oscilloscope.

Figure 21 shows a typical pressure waveform. The pressure rose slowly after trigger for a period of time, then suddenly increased rapidly at a certain point, reached its maximum and finally dropped gradually. We define ignition delay time as the interval between trigger and the moment at which the pressure rises to 10% of its maximum value. Pressure rise time is defined as the interval between moments at which pressure rises to 10% and 90% of its maximum value.

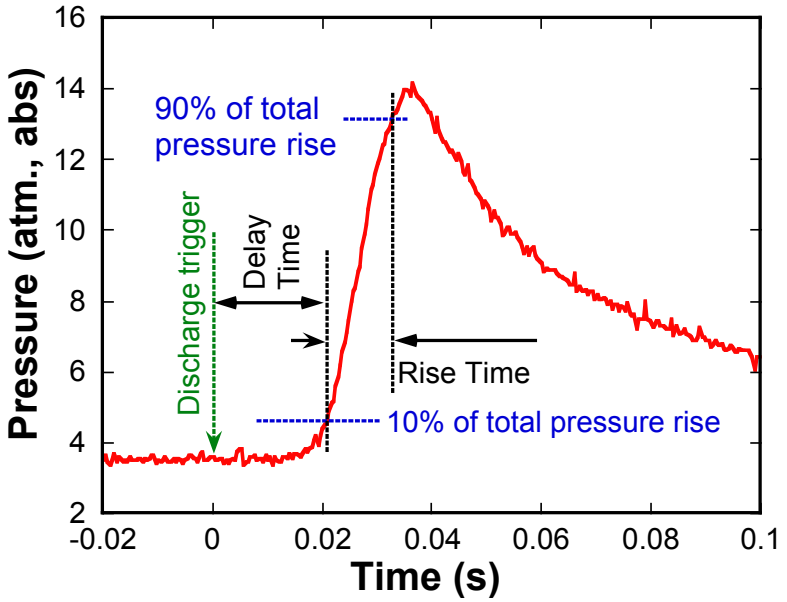

Figure 21. Typical pressure waveform with definitions of ignition delay time, pressure rise time and peak pressure.

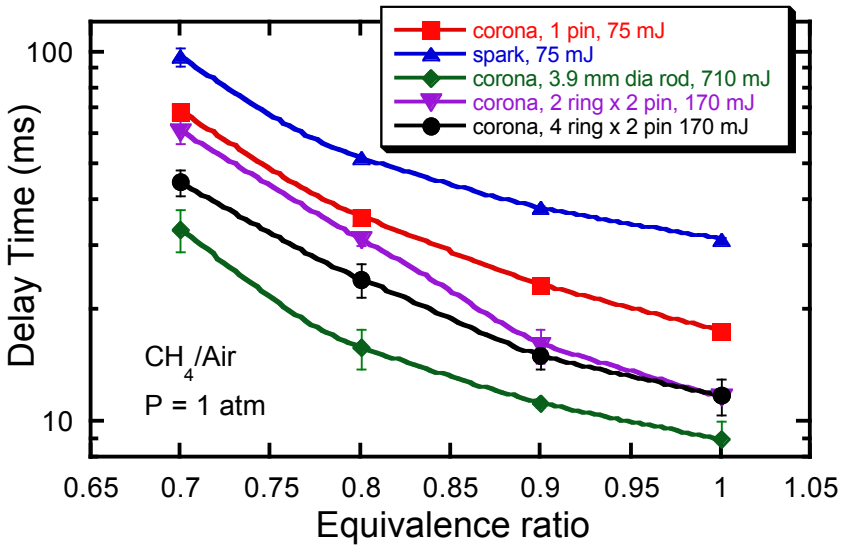

Figure 22. Delay time versus equivalence ratios for corona ignition with various electrode geometries, and comparison with spark ignition.

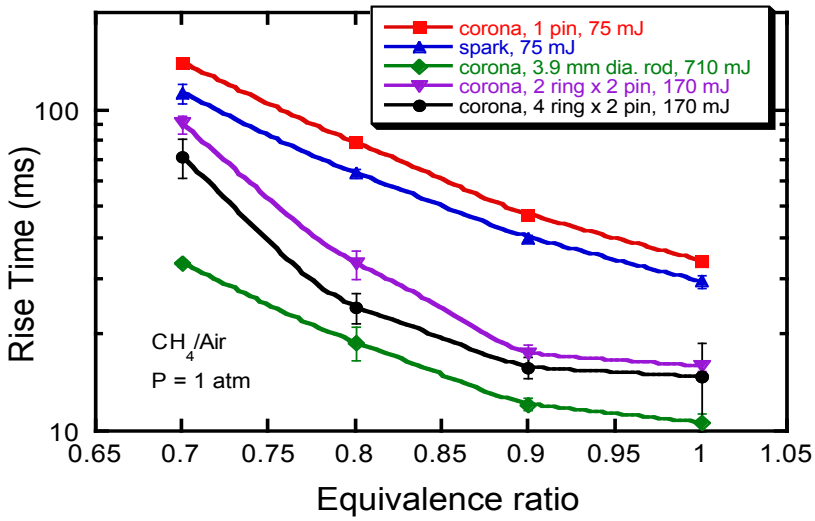

Figure 23. Rise time versus equivalence ratios for corona ignition with various electrode geometries, and comparison with spark ignition.

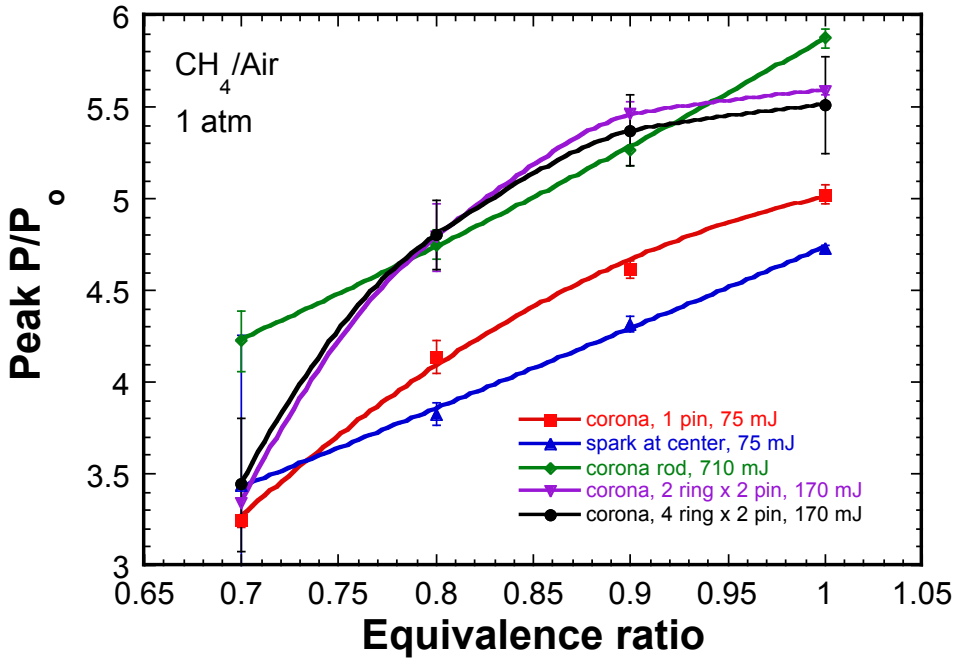

Figure 24. Rise time versus equivalence ratios for corona ignition with various electrode geometries, and comparison with spark ignition.

Figure 22 shows the delay time as a function of equivalence ratio, electrode geometry and discharge type (spark or corona) in the coaxial cylinder. The superiority of the corona ignition or spark ignition can be seen, and the maximum improvement occurs for the rod electrode as compared to the various pin-type electrode. Similar tendencies are found in curves of rise time (Fig. 23) and peak pressure (Fig. 24).

In the engine-like test cylinder, several different electrode geometries were tested in the engine cylinder test chamber, a ring shaped electrode, a straight electrode and a single pin point electrode. The ring electrode allowed the most electrical energy to be deposited to the gas before arcing so it was used for the corona combustion tests. Due to the smaller chamber size of the engine cylinder test chamber the center electrode is much closer to the chamber walls than in the larger cylindrical test chamber and is more likely to arc. Arcing usually occurs at the tip of the electrode or at a sharp bend. In order to prevent the electrode from arcing the end of the electrode was insulated. Without this insulation the energy of the corona was too low to ignite the air/fuel mixture in the cylinder.

Figure 25 shows the pressure rise time in the engine cylinder test chamber for corona only ignition, corona plus arc and for a conventional spark plug. It can be seen that the corona ignition delivers a steeper pressure rise than the conventional spark plug and a higher peak pressure. When the power was increased to allow the corona to arc the peak pressure was higher than the corona alone but it comes at the expense of additional electrical energy needed to produce the arc.

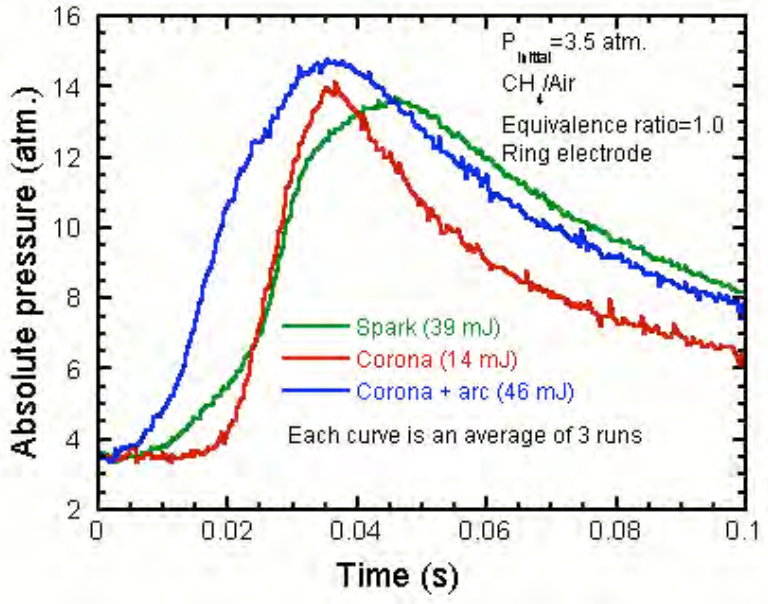

Figure 25. Plot of Pressure vs. Time for Corona, Corona + arc and conventional spark plug with associated electrical energy. Tests performed in engine cylinder test chamber.

3.3 Tests in turbulent, constant-volume chambers

While the mechanisms determined by us to be responsible for the improvements of transient plasma ignition in quiescent mixtures should carry over to turbulent conditions, we felt it was necessary to prove this point to lay any doubt to rest. Previously, it could have been argued that with turbulence, all flames will burn quickly and that the benefit of transient plasma ignition would be lost, but the results below discredit this superfluous argument. To test the effect of turbulence on the benefit of transient plasma ignition, one of our existing cylindrical transient plasma ignition systems (Fig. 3) was used. Exactly the same apparatus was used for all tests (plasma and spark, quiescent and turbulent). The turbulence intensity (u') was about 1 m/s, about 2.5 times the laminar burning velocity (S_L) of stoichiometric hydrocarbon-air flames. Thus, the effect of turbulence on burning velocity should be substantial. Figure 26 shows that (as expected) the turbulent cases have faster rise times, higher peak pressures and faster decay (due to heat losses) in the burned gas. The

results are reasonably repeatable, even though the mixtures are turbulent. The delay times are about the same with or without turbulence for both transient plasma and spark (transient plasma vs. spark affects delay time, but turbulent vs. quiescent does not), thus transport does not play a significant role on delay time. The rise times are faster with transient plasma than with spark, for both turbulent and quiescent cases. Most importantly, *the "improvement factor" (ratio of transient plasma rise time to spark rise time) is nearly the same with or without turbulence.* So the advantages of transient plasma ignition still occur in turbulent flames. The peak pressures are significant higher with transient plasma than with spark, for both turbulent and quiescent cases. In a 'real' combustor, burning faster using transient plasma ignition in the presence of strong turbulence and thus strong heat losses could yield significantly higher thermal efficiency due to the higher peak pressures. Figure 28 (right) shows that similar but even more pronounced trends are exhibited for lean mixtures because of their lower S_L.

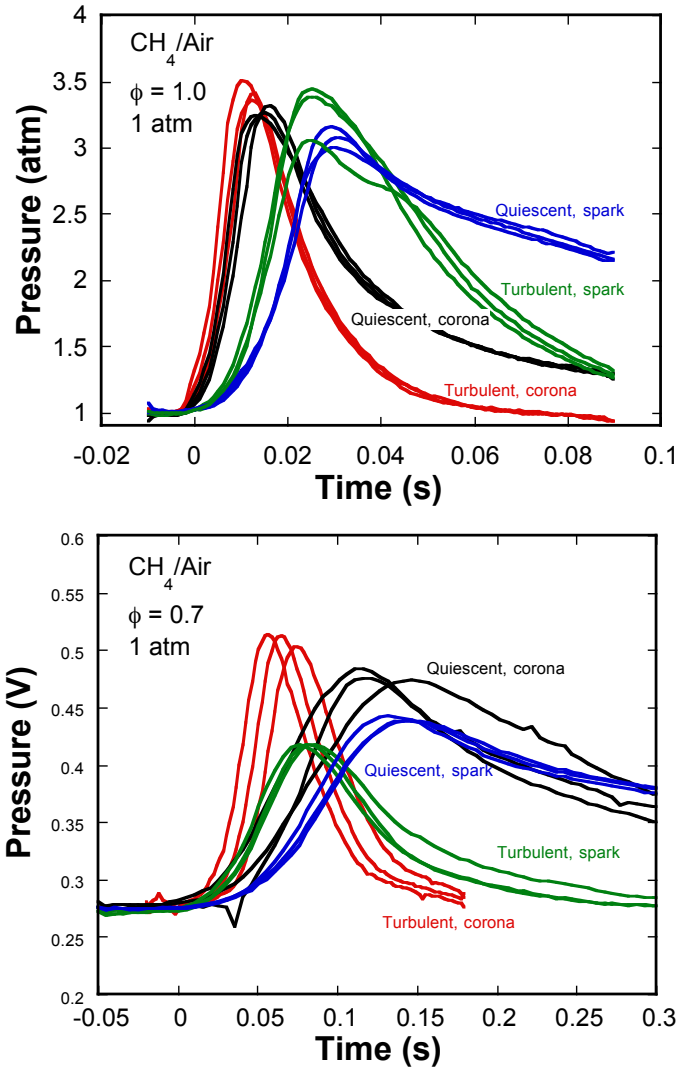

Figure 26. Pressure-time histories of spark-ignited and plasma-ignited quiescent and turbulent flames. Top: stoichiometric mixture; bottom: lean mixture.

3.4 Engine tests

With these encouraging results, tests were conducted using a 2000 Ford Ranger 2.5 liter dual-plug engine running on natural gas. As discussed in the Experimental Apparatus section , one cylinder was fitted with the TPI electrode in one plug port. The same discharge generator used for bench testing was also used for on-engine testing. The other spark plug port was fitted with a modified spark plug containing a Kistler pressure transducer. This cylinder's exhaust gas was collected and analyzed using a Horiba emissions bench. An optical encoder was used to measure crank angle information and in concert with the cylinder pressure data to create P-V diagrams. The plasma electrode was a simple "spike" design, home-built from a modified commercial spark plug; we expect greater improvements may result with more sophisticated electrode designs.

Figures 27 - 29 show, respectively, the P-V diagram, heat release rate and total integrated heat release (not including any heat loss model, which accounts for the drop during expansion) for a typical (not "best case") spark-ignited and plasma-ignited engine cycle. Note that the peak pressure, peak burn rate, total burn duration and peak gas thermal energy (i.e. peak on the heat release curve) are substantially higher for the plasma-ignited than the spark-ignited cycle. The indicated thermal efficiencies are 33.6% and 29.3%, indicating a 33.6/29.3 – 1 = 15% improvement. The improvement is brake efficiency is even larger, about 21%, since a constant friction loss must be subtracted from the indicated work to obtain the brake work. Note also that at the end of the expansion stroke, the "total heat release" has dropped about 40%, meaning that about 40% of the thermal energy generated by combustion was lost to the cylinder walls. Figure 30 is a comparison of "envelope" of brake specific NO_x emissions vs. indicated efficiency for spark-ignited and transient plasma ignited engines. Clearly the tradeoff is more favorable for plasma ignition in that there are points to the "southeast" of any points on this plot for spark ignition. Figures 31 and 32 show that CO and hydrocarbon emissions are similar for the two modes of ignition.

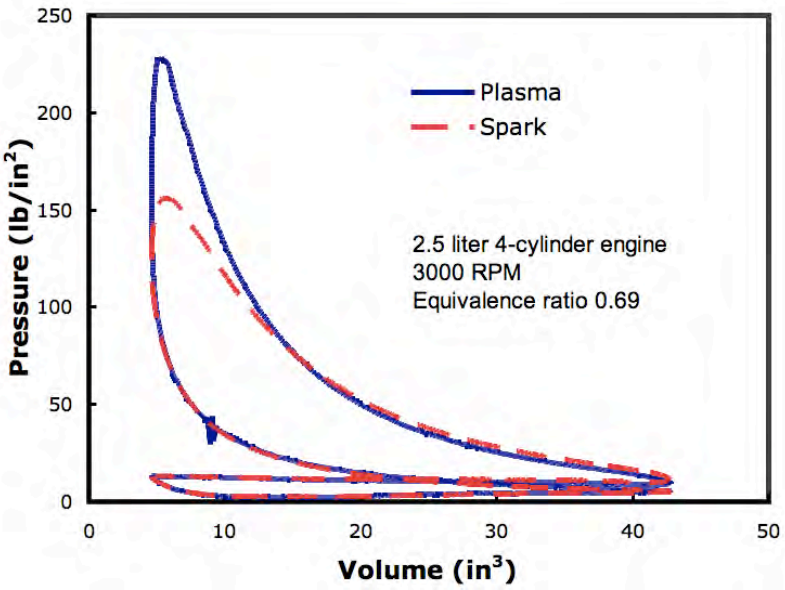

Figure 27. Engine test results (natural gas fuel): typical (not "best case" comparison of spark-ignited and plasma-ignited P-V diagrams.

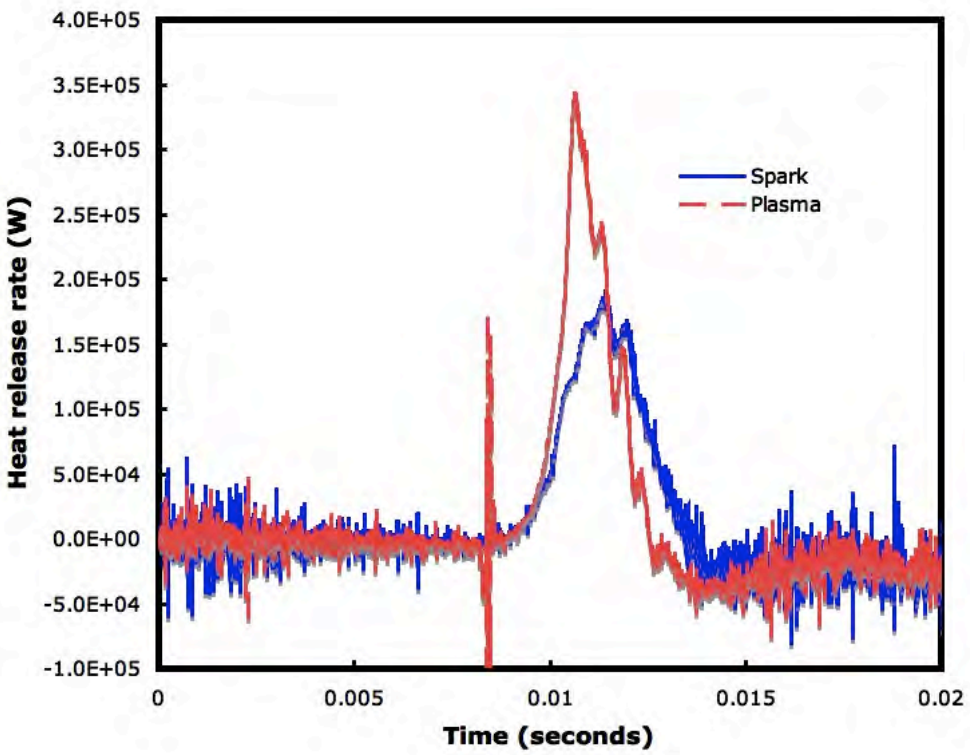

Figure 28. Engine test results (natural gas fuel): gross heat release rate profile (no heat loss model has been incorporated, thus values indicate (heat generation by combustion) – (heat loss/gain to cylinder walls)).

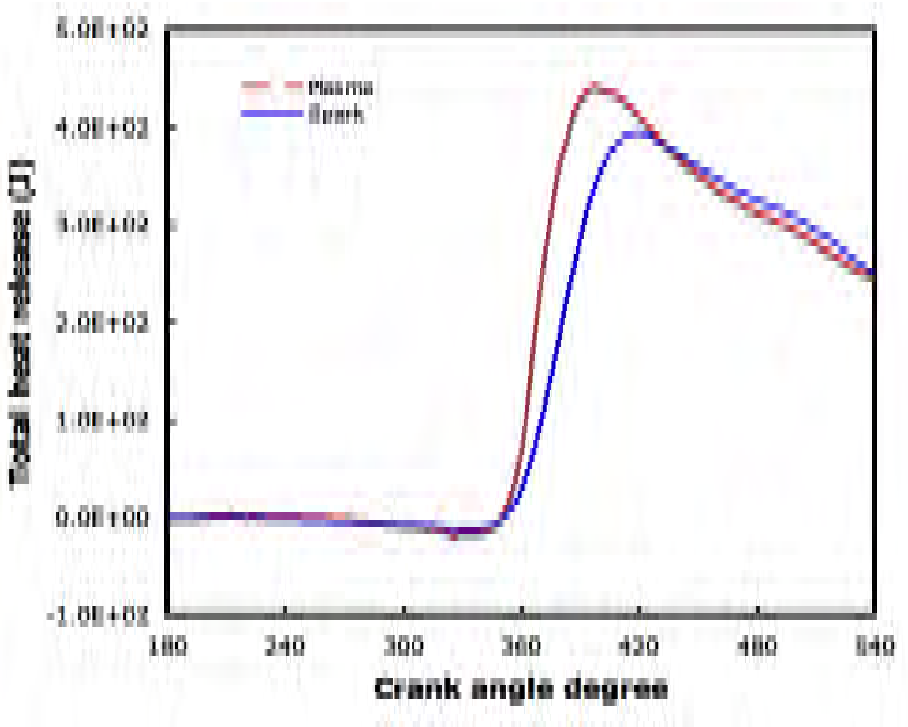

Figure 29. Engine test results (natural gas fuel): integrated heat release rates.

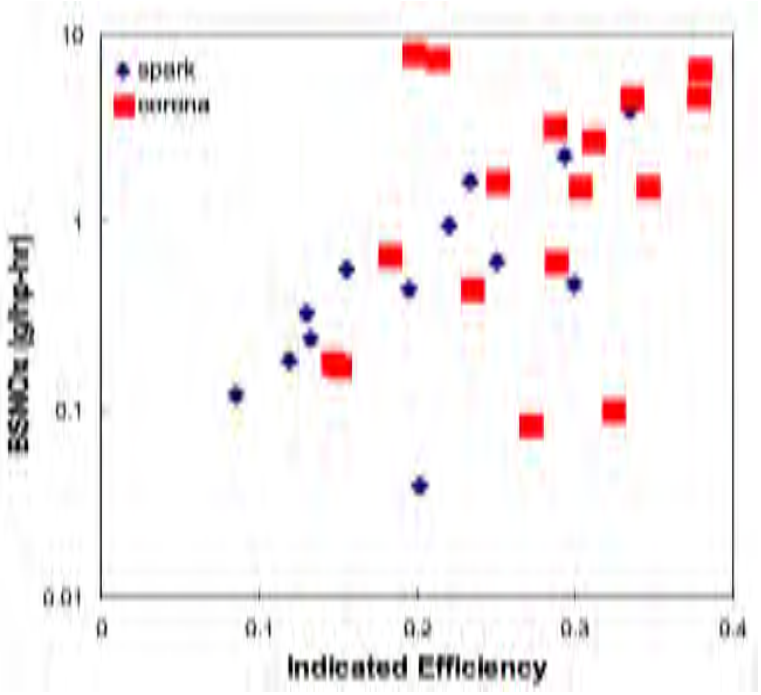

Figure 30. Engine test results (natural gas fuel): comparison of "envelope" of brake specific NO_x emissions vs. indicated efficiency for spark-ignited and transient plasma ("corona") ignited engines.

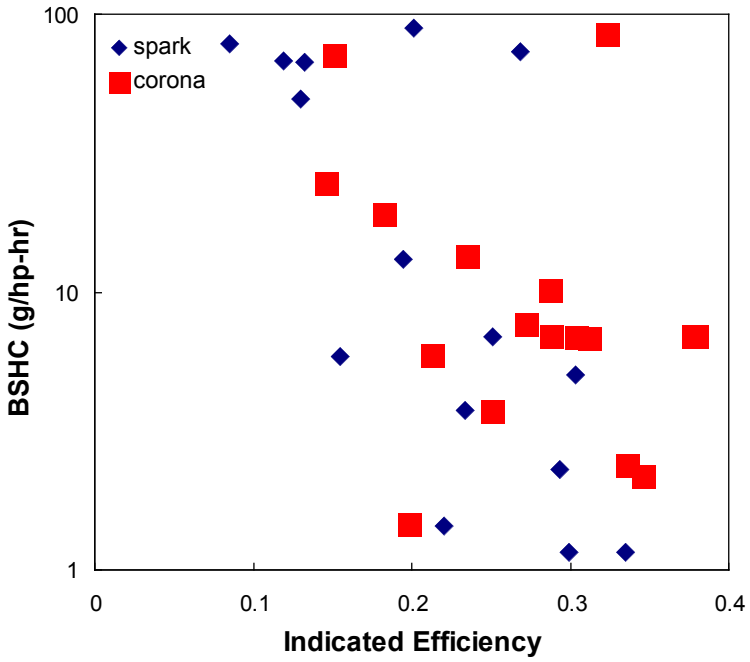

Figure 31. Engine test results (natural gas fuel): comparison of "envelope" of brake specific hydrocarbon emissions vs. indicated efficiency for spark-ignited and transient plasma ("corona") ignited engines.

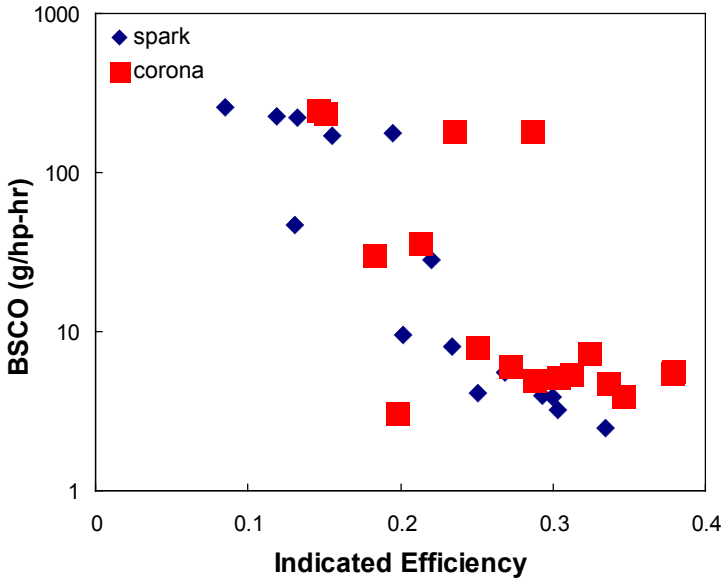

Figure 32. Engine test results (natural gas fuel): comparison of "envelope" of brake specific CO emissions vs. indicated efficiency for spark-ignited and transient plasma ("corona") ignited engines.

4 Conclusions and recommedations

Flame ignition by transient plasma ("pulsed corona") discharges is a promising technology for ignition of natural-gas fueled internal combustion engines. Constant-volume chamber laboratory experiments show that such discharges yield shorter ignition delay and rise times (thus shorter burn times) than flames ignited by conventional sparks under otherwise identical conditions. The rise time is a more significant issue because unlike delay time, rise time can't be compensated by "spark advance" in IC engines. The benefits of corona discharges were also found to apply to turbulent flames in constant-volume chambers. Based on this groundwork, a corona ignition system was tested in an IC engine. For identical conditions, corona ignition was found to yield significantly higher Indicated Mean Effective Pressure (IMEP) for same conditions with same or better Brake Specific NO_x ($BSNO_x$) emissions than spark-ignition, with comparable CO and hydrocarbon emissions. Cylinder pressure analysis showed that corona ignition yielded shorter burn times and faster heat release rates than spark ignition at identical engine operating conditions.

5 Implementation

Transient plasma ignition is an attractive technology for the ignition of small internal combustion engines because of engine data showing significant reductions in ignition delay, ignition of leaner fuel-air mixtures, lower specific fuel consumption, and faster burn rates. The inherently faster burn rates produced by Transient plasma ignition may be used in conjunction with intake port and combustion chambers intentionally shaped to provide reduced turbulence levels and thus reduce thermal losses while still obtaining rapid burn rates. Moreover, the reduced cooling system load means that smaller cooling systems can be used, thus reducing aerodynamic drag. This double benefit (increased efficiency and reduced drag) is potentially enabling technology for long-distance small engines having large combustion chamber surface area to volume ratios.

6 Publications

Singleton DR, Sinibaldi JO, Brophy CM, Kuthi A, Gundersen MA, "Compact Pulsed-Power System for Transient Plasma Ignition," IEEE TRANSACTIONS ON PLASMA SCIENCE, Volume 37, Pages 2275-2279 (2009)

Shiraishi, T; Urushihara, T; Gundersen, M, "A trial of ignition innovation of gasoline engine by nanosecond pulsed low temperature plasma ignition," JOURNAL OF PHYSICS D-APPLIED PHYSICS, Volume 42, Article Number 135208 (2009)

Singleton, D; Cathey, C; Kuthi, A, Gundersen, M., "Applications of Power Modulator Technology to Ignition and Combustion," PROCEEDINGS OF THE 2008 IEEE INTERNATIONAL POWER MODULATORS AND HIGH VOLTAGE CONFERENCE, Pages 174-177 (2008).

Cathey, C; Cain, J; Wang, H, Gundersen, M., "OH production by transient plasma and mechanism of flame ignition and propagation in quiescent methane-air mixtures," COMBUSTION AND FLAME Volume 154 Pages 715-727 (2008).

Tang, T; Singleton, DR; Cathey, CD, Gundersen, M. A., "Solid state pulse adding system for transient plasma ignition," 2007 IEEE PULSED POWER CONFERENCE, Pages 995-999 (2007).

Cathey, CD; Tang, T; Shiraishi, T, Gundersen, M., "Nanosecond plasma ignition for improved performance of an internal combustion engine," 3rd International Workshop and Exhibition on Plasma-Assisted Combustion, IEEE TRANSACTIONS ON PLASMA SCIENCE Volume 35 Pages 1664-1668 (2007).

Memarzadeh, S., Rossi, J. Neiman, R, Ronney, P. D., Gundersen, M. A., "Transient Plasma Ignition for Internal Combustion Engines," 2007 U. S. National Meeting, Combustion Institute, La Jolla, CA, March 26 – 28, 2007.